

**NATIONAL RADIO ASTRONOMY OBSERVATORY
GREEN BANK, WEST VIRGINIA**

ELECTRONICS DIVISION TECHNICAL NOTE NO. 176

Title: TCHEB_x: Homogenous Stepped Waveguide Transformers

Authors: E. Wollack

Date: November 11, 1995

DISTRIBUTION:

GB

GB Library
G. Behrens
E. Childers
R. Fisher
J. Ford
W. Grammar
R. Lacasse
R. Norrod
D. Parker
D. Schiebel
M. Stennes
T. Weldon
S. White

CV

ER Library
IR Library
M. Balister
N. Bailey
R. Bradley
C. Burgess
L. D'Addario
R. Escoffier
N. Horner
A. R. Kerr
S.-K. Pan
M. Pospieszalski
S. Srikanth
A. R. Thompson
E. Wollack

TU

Library-Downtown
Library-Mountain
R. Freund
J. Payne
A. Perfetto
W. Shillue

VLA

AOC Library
L. Beno
W. Brundage
J. Campbell
C. Janes
R. Latasa
P. Lilie
P. Napier
P. Rhodes
R. Sramek
R. Weimer

TCHEB_x: Homogenous Stepped Waveguide Transformers

E. Wollack
NRAO, Charlottesville, VA
November 11, 1995

1. Introduction

TCHEB_x is a design tool for the synthesis of homogenous stepped transformer prototypes with Tchebyshev weights. This set of subroutines is a straightforward implementation with first order accuracy in the junction reflection coefficients [4, 5, 12, 15]. The user specifies the desired bandpass $f_{o1} < f < f_{o2}$ relative to the cutoff frequency f_c , the number of transformer sections N , and the desired input and output guide dimensions. The transformer dimensions computed with the algorithm agree ¹ with those obtained with the tables of Matthaei, Young, and Jones [8] to a few parts in 10^4 . Design examples are given along with typical measured data.

2. Rectangular Waveguide Transformers

A homogenous TE₁₀[□] transformer has a constant broadwall dimension, a_o , and varying guide heights, b_i (see Figure 1). The constant broadwall dimension results in a guide dispersion along the direction of propagation which is independent of position or "homogeneous" throughout the structure. The steps in guide height are used to produce the desired reflection amplitude taper. The section lengths are nominally

$$l_o \equiv \lambda_{go}/4 = \frac{\lambda_{g1}\lambda_{g2}}{2(\lambda_{g1} + \lambda_{g2})}, \quad (1)$$

where λ_{g1} and λ_{g2} are the guide wavelengths evaluated at the band edges. Thus, the structure is synchronously tuned at frequency

$$f_o/f_c = \sqrt{1 + \left(\frac{a_o}{2l_o}\right)^2}. \quad (2)$$

The number of sections N , normalized fractional bandwidth

$$w_q \equiv \frac{2(\lambda_{g1} - \lambda_{g2})}{\lambda_{g1} + \lambda_{g2}}, \quad (3)$$

and transformer impedance ratio

$$R_o \equiv Z_{N+1}/Z_o = b_{N+1}/b_o, \quad (4)$$

¹If higher precision is required, for $N < 6$ sections, Alison's [1] polynomial evaluation of the junction weights is recommended. One cautionary note in the limit of vanishing reflection coefficient magnitude: the reflection due to the junction discontinuity must be small compared to the reflection due to the impedance step for the first order treatment to be valid. In practice, this limitation can be circumvented by synthesizing the desired junction reflection coefficients by successive approximation or gradient search (see, *e.g.*, [3]).

determine the voltage standing wave ratio of the transition over the pass band. For a Tchebyshev taper, the maximum in band reflection is approximately

$$\text{VSWR} \simeq 1 + \ln(R_o) \frac{T_N\left(\frac{\cos(\phi)}{\cos(\phi_o)}\right)}{T_N\left(\frac{1}{\cos(\phi_o)}\right)} < 1 + \frac{\ln(R_o)}{T_N\left(\frac{1}{\cos(\phi_o)}\right)}, \quad (5)$$

where T_N is a Tchebyshev polynomial of order N , $\phi_o = (2 - w_q)\pi/4$ is the electrical length at the lower band edge, ϕ is the electrical phase between steps, and it is assumed $R_o < (2/w_q)^{N/2}$ [8]. The non-ideal performance of the step junctions is compensated by correcting the section lengths [4, 8, 14] as outlined in Section 3. An example input data file and the resulting design are outlined in Section 4. The performance of typical designs is presented in Figure 4.

3. Transformer Section Length Estimates

For a small E-plane step, the discontinuity in waveguide cross-section only has a second order effect on the junction VSWR. The presence of the discontinuity is equivalent to an additional phase shift. To minimize the total junction reactance, symmetrical steps are preferred.

For an H-plane step, in addition to the phase perturbation introduced by the non-ideal junction, there can be a significant perturbation on the junction reflection coefficient [16]. The presence of the step increases the effective impedance ratio between the two guides. If H-plane steps $> 10\%$ are used, the first order treatment fails. As the guide approaches cutoff, larger H-plane steps can be accommodated.

If both E- and H-plane steps are required, the total energy stored at the junction should be minimized. This will reduce the loss and dispersion [8, p. 344]. The normalized junction susceptances are computed as follows (see Figure 2):

(a) Susceptance of an Abrupt E-Plane Step [7, (pp. 307–310)]:

$$b_{Ei} \equiv \frac{B_{Ei}}{Y_i} \approx \frac{2b_i}{\lambda_g} \left(\frac{\beta}{2}\right)^2 \left[\frac{2 \ln \frac{2}{|\beta|}}{1 - \beta} + 1 + \frac{17}{16} \left(\frac{b_i}{\lambda_g}\right)^2 \right] + \dots \quad (6)$$

where $\beta \equiv (1 - b_{i-1}/b_i) \ll 1$, and $\lambda_g = 2\lambda_{gi-1}\lambda_{gi}/(\lambda_{gi-1} + \lambda_{gi})$. In a homogenous structure, $\lambda_g = \lambda_{go}$, in each section.

(b) Susceptance of an Abrupt H-Plane Step [7, (pp. 296–304)²]:

$$b_{Hi} \equiv \frac{B_{Hi}}{Y_i} \approx -\frac{\lambda_{gi}}{2a_i} \left(\frac{\alpha^2 (1 + \alpha) \ln \frac{2}{|\alpha|}}{1 - \frac{\alpha}{2}} \right) \left[1 - \frac{27}{8} \left(\frac{Q_{i-1} + Q_i}{1 + 8 \ln \frac{2}{|\alpha|}} \right) \right] + \dots, \quad (7)$$

²Consider Equation 1c [7] in the limit where the two guides have approximately the same broadwall dimension $a \simeq a'$ (i.e., $\beta \equiv 1 - a'/a \rightarrow 0$). The impedance ratio for the two guides should reduce to

$$\frac{Z'_o}{Z_o} \rightarrow \frac{(\eta b' \lambda'_g / a' \lambda_o)}{(\eta b \lambda_g / a \lambda_o)} = \frac{a \lambda'_g}{a' \lambda_g}$$

where λ_g and λ'_g are the guide wavelengths in the two rectangular sections (see [7], Figure 5.24-1). This would suggest that $\lambda'_g a' / \lambda_g a$ should be replaced by $\lambda'_g a / \lambda_g a'$ in Equations 1a, 1b. and 1c. Also, see the discussion in [9].

where $\alpha \equiv (1 - a_{i-1}/a_i) \ll 1$, $Q = 1 - \sqrt{1 - (2a/3\lambda_o)^2}$, and λ_o is the free-space wavelength which corresponds to the transformer synchronous frequency. For a pure H-plane step, we note the following: the effective impedance ratio is greater than the ratio of the section's characteristic impedances [9]. In addition, the guide wavelength changes and the terminal plane shifts out of the plane of the junction. These undesirable effects provide a strong motivation to keep α as small as possible. In order for the transformer sections to maintain the desired phase relationship over the design bandwidth, an approximately homogenous structure is desirable.

The reference plane corrections to the section lengths are applied by uniformly weighting the junction's susceptance due to the E- and H-plane steps. With this convention, the corrected length of the i^{th} section can be approximated by

$$l_i \simeq \frac{\lambda_{gi}}{4} \left(1 - \frac{2}{\pi} (|\delta\phi^- + \delta\phi^+|_{i+1} - |\delta\phi^- - \delta\phi^+|_i) \right) + \dots, \quad (8)$$

as described in [8], where the phase shift

$$\delta\phi_i^\pm \simeq \frac{1}{2} \tan^{-1} \left(\frac{|b_{Ei}| - |b_{Hi}|}{\frac{Z_i}{Z_{i-1}} \pm 1} \right) + \dots, \quad (9)$$

is small compared to one radian. This physically corresponds to weighting the first order phase shift for each plane by its stored energy. For a homogenous rectangular transformer, there are no steps in guide width and $b_i^H = 0$. In a transformer with inhomogenous cross-section, the capacitance due to changes in height can be compensated by corresponding inductive steps in width at each junction [3, 20]. It is important to keep in mind, however, for this simplistic circuit model to approximate reality, the impedance ratio resulting from the H-plane steps must essentially be unity. Further refinement of the transformer's response can be realized through the use of a full-wave analysis for optimization (see, *e.g.*, [2, 11]).

4. TCHEB_X: Homogenous Transformer Design Example

(a) Input Data File: TCHEB_X.IN

```
4      0.4200  0.1700  0.4200  1.2200  1.9800
```

(b) Output Data File: TCHEB_X.OUT

Number of sections	(N):	4
Lower band edge	(fo1/fc):	1.22000
Upper band edge	(fo2/fc):	1.98000
Design frequency	(fo/fc):	1.56504
Fractional bandwidth	(wq):	0.83900
Transformer impedance ratio (Ro):		2.47059
Max in-band VSWR	(VSWR):	1.02472

Section (i)	Width (a _i)	Height (b _i)	Length (l _i)
0	0.42000	0.17000	0.17443
1	0.42000	0.18563	0.16774
2	0.42000	0.23129	0.16583
3	0.42000	0.30870	0.16884
4	0.42000	0.38464	0.17820
5	0.42000	0.42000	0.17443

5. Rectangular-to-Circular Waveguide Transitions

Let us briefly consider the TE_{10}^{\square} – to – TE_{11}° waveguide transition reported in the literature by Bathker [25]. This transition plays two roles—it acts as a mode converter and it transforms the impedance level between the two guides. The transition is designed as follows: To minimize the effect of guide dispersion between the sections and simplify the design, a constant cutoff is maintained throughout the structure. For the rectangular and circular guides, the cutoff wavelengths for the dominant modes are $\lambda_c(TE_{10}^{\square}) = 2a$ and $\lambda_c(TE_{11}^{\circ}) = 2\pi r/s_{11}$, respectively, where a is the rectangular guide broadwall dimension, r is the cylindrical guide radius, and $s_{11} = 1.841184$ (see Figure 3). Equating the input and output cutoff wavelengths, we obtain the constant cutoff radius. $r_{\text{pyle}} = a_o s_{11}/\pi$ [23].

The normalized rectangular waveguide impedance in the power-voltage basis is $Z_i \equiv 2b_i/a_i$, where a_i and b_i are respectively the i^{th} section’s width and height. For sections with truncated corners³, the height and width are varied with constant section impedance while searching for the cross-section which maintains a constant cutoff in the structure. We use the Rayleigh-Ritz procedure [10] to numerically estimate the eigenvalues in the truncated sections. To minimize the error in the eigenvalue determination, the dominant mode rectangular guide eigenfunction is used as the trial function for sections $i = 2, 3$ and the dominant cylindrical eigenfunction is used for $i = 4$. Bathker’s measured data is presented in Figure 5 along with a finite element calculation of the reported structure’s return loss. The results of the synthesis outline here are also displayed and are referred to as “Corrected Eigenvalue” in the figure. The normalized dimensions for both transition designs are given in Table 1.

This algorithm is unable to exactly reproduce the dimensions given in Bathker’s Table 1. Several comments are in order: 1.) For a $R_o = 2.0$ transformer ratio and normalized fraction bandwidth of $w_q = 0.8$, the observed response is 12 to 18 dB higher than the sidelobe level in an ideal Tchebyshev taper. In addition, the response does not have the correct placement of the nulls and maxima in the passband (*i.e.*, there should be $N = 4$ zeros—the data suggest that significant phase and amplitude

³The corners are truncated if the width and height for the i^{th} section exceed the boundary defined by the circular waveguide, $r_{\text{pyle}}^2 < (a_i/2)^2 + (b_i/2)^2$ [26]. Inserting the expression for the normalized guide impedance, we find for $Z_i/2 > \sqrt{(2s_{11}a_o/\pi a_i)^2 - 1} \simeq 0.61$, the transformer sections are truncated.

TABLE 1
STEPPED TE_{10}^{\square} – to – TE_{11}° WAVEGUIDE TRANSITIONS

	Section i	Width a_i [a_o]	Height b_i [a_o]	Length l_i [a_o]	Cross-section Type
Bathker [25]	0	1.0000	0.5000	0.4288	Rectangular
	1	1.0000	0.5337	0.4119	Rectangular
	2	1.0007	0.6326	0.4028	Rectangular
	3	1.0195	0.8065	0.4142	Truncated, $2r/a_o = 1.1721$
	4	1.0786	1.0107	0.4281	Truncated, $2r/a_o = 1.1721$
	5	1.1721	1.1721	0.4288	Cylindrical, $2r/a_o = 1.1721$
Corrected Eigenvalue	0	1.0000	0.5000	0.4288	Rectangular
	1	1.0000	0.5335	0.4135	Rectangular
	2	1.0009	0.6326	0.4098	Truncated, $2r/a_o = 1.1721$
	3	1.0209	0.8079	0.4151	Truncated, $2r/a_o = 1.1721$
	4	1.0558	0.9828	0.4349	Truncated, $2r/a_o = 1.1721$
	5	1.1721	1.1721	0.4288	Cylindrical, $2r/a_o = 1.1721$

The mode transducer dimensions are expressed in terms of the input rectangular guide broadwall, a_o . The computed section length and cross-section dimensions are uncertain by approximately ± 0.003 for the corrected eigenvalue synthesis. The additional significant figures given in the table indicate the geometry modeled.

errors are present in the taper). 2.) The eigenvalues used in [23, 25] are forced to match those of rectangular and cylindrical guides at the endpoints by imposing a $\{1 - \sin^4\}$ weighting. 3.) The exact section length correction is stated to be, “based on weighting the length corrections according to E- and H-plane susceptance magnitudes...[25].” In the small reflection limit, the junction phase shifts are $\ll \pi/4$. Under these conditions, weighting the phase shifts with the susceptance magnitude reduces to a uniform weighting of the phase shifts computed for the two planes.⁴ 4.) Although the impedance basis is “rigorously consistent with the power-voltage...for the dominant mode rectangular and cylindrical waveguides...[25].” this condition is not met in the presence of the stepped junctions required to maintain constant cutoff. This can be physically seen by noting that an H-plane step has a non-trivial turns ratio [9, 16] (*i.e.*, such a junction is inherently a transformer with a turns ratio greater than the ratio of guide impedances). This effectively increases the total impedance ratio required for the transition. 5.) The junction reactances have been ignored in the design procedure. Since the Pyle condition fixes the relation between the input and output guide geometry, this effectively increases the required transformer ratio by the product of the excess VSWR’s resulting from the junction reactances.

⁴Recall the susceptance is proportional to the phase shift in the small angle approximation. The weighted junction phase shift is $\langle \phi \rangle \approx (\phi_E^2 - \phi_H^2)/(\phi_E + \phi_H) = \phi_E - \phi_H$. If one looks at the capacitive/inductive corrections stated in [25], the section lengths reported are consistent with an infinite E-plane weight for all sections except for $i = 3$ (?). In Padman [26], a similar weighting scheme is more concisely described. However, in computing the junction phase shifts, the admittance ratios are given as $Y_{i+1}/Y_i = b_i/b_{i+1}$ for both E- and H-plane steps (TE_{10}^{\square} illumination). For internal consistency, this should read $Y_{i+1}/Y_i = b_i a_{i+1} \lambda_{gi}/b_{i+1} a_i \lambda_{gi+1}$. In the absence of a closed-form expression for the susceptance of a truncated guide junction with sufficient accuracy, we estimated l_3 and l_4 from finite element calculations for the corrected eigenvalue taper design.

These observations suggest some degree of caution must be exercised in using the design synthesis outlined by Bathker. The cumulative effects of the mechanisms outlined above are estimated to increase the effective transformer ratio to $R_o \approx 2.6$. This suggests that a 0 to 6 dB improvement in the return loss to the corrected design might be expected (notice the null at the low end of the band is washed out and the sidelobe distribution is unequal for the corrected eigenvalue design) from further refinement of the synthesis procedure. From a fabrication and computational standpoint, however, increasing the return loss to ~ -35 dB and correspondingly adjusting the fractional bandwidth might result in a more productive design goal (alternatively, the number of steps should be increased to $N = 5$). A summary of circular-to-rectangular transitions of potential interest is given in the bibliography.

6. A Comment Regarding Impedance Concepts in Guiding Structures

The generalized impedance concept allows the machinery historically developed for TEM transmission line synthesis to be used for waveguide structures [13]. Three definitions are commonly used in guiding structures for the average impedance:

$$Z_{PI} \equiv 2P/I^*I$$

$$Z_{VI} \equiv V/I$$

$$Z_{VP} \equiv V^*V/2P$$

where,

$$P = \frac{1}{2} \int \int_S (\vec{E} \times \vec{H}^*) \cdot d\vec{S}$$

is the power flux through the guide cross-section S ,

$$I = \oint_C (\hat{n} \times \vec{H}) \cdot d\vec{l}$$

is the longitudinal current flow in a closed path C around the port (the net current flow through the port is zero, the current of interest is the average of the absolute value of the current flowing into and out of the port), and

$$V = \max \left\{ \int_A^B (\vec{E} - (\vec{E} \cdot \hat{n}) \cdot \hat{n}) \cdot d\vec{l} \right\}$$

is the peak voltage across the cross-section (A and B are the points on the port where the potential difference is maximized). These relations satisfy the following: $Z_{PI} < Z_{VI} < Z_{VP}$ and $Z_{VI} = (Z_{PI}Z_{VP})^{1/2}$. All three definitions are proportional to the wave impedance, Z_{EH} , of the mode under consideration. See Table 2 for the dominant circular and rectangular guide impedances computed from these definitions.

The ratio of the response to the driving force is the generalized impedance. For a TEM mode, the definitions involving power form upper/lower bounds on the guide's characteristic impedance. For a non-TEM mode, there can be some ambiguity identifying which field parameter plays which role. The magnitude of the impedance presented by the guide cross-section is only determined up to a multiplicative factor dependent upon the details of the definition. Since the topology freely admits the insertion of an ideal transformer, only the scattering parameters are observable. The choice of the "best" impedance basis is intimately related to the symmetry of the guiding structure and

TABLE 2
WAVEGUIDE IMPEDANCE BASIS

Impedance	TE_{10}^{\square}	TE_{11}°
Definition	$[\eta\lambda_g/\lambda_o]$	$[\eta\lambda_g/\lambda_o]$
Z_{EH}	1	1
Z_{PI}	$\pi^2 b/8a$	$\pi(1 - s_{11}^2)/8$
Z_{VI}	$\pi b/2a$	$\int_0^{s_{11}} J_o(x) dx / J_1(s_{11}) - 1$
Z_{VP}	$2b/a$	2

$\eta = (\mu_o/\epsilon_o)^{1/2} \simeq 377\Omega$ is the intrinsic impedance of free-space.

the discontinuities present in the system. For the single mode integrated impedance concept to be valid, the mode's symmetry should only be broken along one of the integration paths. In addition, the field distribution on either side of the junction must have the same overall symmetry.

The above definitions can provide useful guidelines for a design in this limit. For example, Z_{PI} is expected to yield useful results when the longitudinal current can be uniquely defined (*e.g.*, with TE_{10}^{\square} illumination—a change in guide width or a slot-like perturbation), Z_{VP} is a good impedance basis when a potential can be uniquely defined (*e.g.*, changes in guide height or a strip-like perturbation), and Z_{VI} is useful for structures where the potential and the longitudinal current are both uniquely defined (*i.e.*, TEM mode). In expressing the effect of a waveguide junction in terms of the observable scattering parameters, we note that the above definitions are physically equivalent to expressing the dominant mode impedance in terms of the appropriate cross-section average and the higher order terms as a lumped reactance. Since all measurable quantities appear *as impedance ratios*, if the symmetry implied by the basis is present, the details orthogonal to the discontinuity drop out.

This may be the origin of the common assertion that the exact impedance basis is unimportant as long as the same definition is used throughout the calculation. Strictly speaking, this implies a level of symmetry which may not be present.⁵ Since the averaging process is not unique, it is quite easy for the details of the impedance definition to erroneously appear in a calculation of the observable parameters.⁶ In structures with low symmetry, these simple averaging procedures cannot *a priori* be expected to accurately represent the generalized impedance at each *junction*. To accurately predict the behavior of the entire *structure*, a full analysis of the relevant modes is required (see, *e.g.*, the techniques outlined in [27]).

⁵In a complete modal description, two of the following conditions must be realized: the transverse electric fields are matched, the transverse magnetic fields are matched, or the complex power is conserved. We note that the implied separable nature of the impedance is only approximately achieved under the best of conditions (the form of the impedance matrix is over-constrained). To the extent that the junction symmetry allows this cancellation to occur and the section can be approximated as a scalar (*i.e.*, a single term of a modal expansion), the impedance basis concept is useful.

⁶In a particular basis, the expressions employed to represent the system may simplify or improve convergence; however, the underlying physical outcome does not depend upon the choice of representation. Although the impedance concept outlined is intuitively appealing, it is not necessarily the “natural” parameterization for waveguide scattering problems. In throwing complete rigor aside, we strive to retain the salient features of the underlying physical (and calculable) processes in the hope that the resulting prototype design can be used as a starting point for optimization.

General References:

- [1] Alison, W., "Simplified Procedure for the Design of Multisection Chebyshev Quarterwave Transformers," 1968, *Elec. Let.*, vol. 4, no. 16, pp. 331–332.
- [2] Arndt, F., Tucholke, U., and Wriedt, T., "Computer-Optimized Multisection Transformers Between Rectangular Waveguides of Adjacent Frequency Bands," 1984, *IEEE Trans. on Microwave Theory and Techniques*, vol. MTT-32, no. 11, pp. 1479–1484.
- [3] Bandler, J.W., "Computer Optimization of Inhomogeneous Waveguide Transformers," 1969, *IEEE Trans. on Microwave Theory and Techniques*, vol. MTT-17, no. 8, pp. 563–571.
- [4] Cohn, S.B., "Optimum Design of Stepped Transmission-line Transformers," 1955, *IRE Trans. on Microwave Theory and Techniques*, vol. MTT-3, no. 3, pp. 16–20.
- [5] Collin, R.E., "Theory and Design of Wide-Band Multisection Quarter-Wave Transformers," 1955, *Proc. IRE*, vol. 43, pp. 179–185.
- [6] Hewlett Packard EEsof Division, Hewlett Packard High Frequency Structure Simulator (HFSS), Santa Rosa, CA 95403.
- [7] Marcuvitz, N., *Waveguide Handbook*, 1986, Peter Peregrinus, London (E/H-plane step junctions in rectangular guide: 296–304, 307–310).
- [8] Matthaei, G., Young, L., and Jones, E., *Microwave Filters, Impedance-Matching Networks and Coupling Structures*, 1964, McGraw-Hill, New York, Chap. 6.
- [9] Miles, J.W., "The Equivalent Circuit for a Plane Discontinuity in a Cylindrical Wave Guide," 1946, *Proc. IRE*, vol. 34, pp. 728–742. (Compare with Marcuvitz expressions for H-plane step.)
- [10] Morse, P.M. and Feshbach, H., *Methods of Theoretical Physics*, 1953, McGraw-Hill.
- [11] Patzelt, H. and Arndt, F., "Double-Plane Steps in Rectangular Waveguides and their Application for Transformers, Irises and Filters," 1982, *IEEE Trans. on Microwave Theory and Techniques*, vol. MTT-30, no. 5, pp. 771–776. (For comments, see Sipila, M.T., vol. MTT-33, no. 11, 1985.)
- [12] Riblet, H.J., "General Synthesis of Quarter-Wave Impedance Transformers," 1957, *IRE Trans. on Microwave Theory and Techniques*, vol. MTT-5, no. 1, pp. 36–43.
- [13] Schelkunoff, S.A., "Impedance Concept in Wave Guides," 1944, *Quarterly of Applied Mathematics*, vol. 2, no. 1, pp. 1–15.
- [14] Uher, J., Bornemann, J., and Rosenberg, U., *Waveguide Components for Antenna Feed Systems: Theory and CAD*, 1993, Artech House, Boston, section 3.2.
- [15] Young, L., "Tables for Cascaded Homogeneous Quarter-Wave Transformers," 1959, *IRE Trans. on Microwave Theory and Techniques*, vol. MTT-7, no. 2, pp. 233–237 (See MTT-8, no. 2, 1960, pp. 243–244 for corrections).
- [16] Young, L., "Optimum Quarter-Wave Transformers," 1960, *IRE Trans. on Microwave Theory and Techniques*, vol. MTT-8, no. 5, pp. 478–482.

Selected Circular-to-Rectangular Transitions:

- [17] Ragan, G.L., *Microwave Transmission Circuits*, 1948, McGraw-Hill, New York, section 6.17. (Survey of adiabatic, mitered, and single step transitions—narrow band designs.)
- [18] Harvey, A.F., *Microwave Engineering*, 1963, Academic Press, pp. 80–81, 102–104, 166–167. (Survey of adiabatic, mitered and multi-step transitions.)
- [19] Robertson, S.D., “Recent Advances in Finline Circuits,” 1956, *IRE Trans. Microwave Theory and Techniques*, vol. MTT-4, no. 4, p. 263–267. (cylindrical-to-rectangular guide finline transformers).
- [20] Ohm, E., “A Broad-Band Microwave Circulator.” 1956, *IRE Trans. on Microwave Theory and Techniques*, vol. MTT-4, no. 4, pp. 210–217.
- [21] Maher, B., “A Stepped-Dielectric Transformer for Rectangular-to-Circular Waveguide,” 1961, *IRE Trans. Microwave Methods and Techniques*, vol. MTT-9, no. 6, pp. 572–573.
- [22] Wolfert, P., “A Wide-Band Rectangular-to-Circular Mode Transducer for Millimeter Waves,” 1963, *IRE Trans. on Microwave Theory and Techniques*, vol. 11, no. 5, pp. 430–431.
- [23] Pyle, J.R., “A Circular-to-Rectangular Waveguide Transition Maintaining a Constant Cutoff Wavelength,” 1964, Australian Defense Scientific Service Weapons Research Establishment, Salisbury, S.A., Tech. Note, PAD 94. (Also see, Pyle, J.R. and Angley, R.J., “Cutoff Wavelengths of Waveguides with Unusual Cross Sections,” 1964, *IEEE Trans. on Microwave Theory and Techniques*, vol. MTT-12, no. 5, pp. 556–557. For correction to parallel eigenvalue case, see Sinnott, *et al.*, “The Finite Difference Solution of Microwave Circuit Problems,” 1969, *IEEE Trans. on Microwave Theory and Techniques*, vol. MTT-17, no. 8, pp. 464–478.)
- [24] Stuchly, S. and Kraszewski, A., “Wide-Band Rectangular-to-Circular Waveguide Mode and Impedance Transformer,” 1965, *IRE Trans. on Microwave Theory and Techniques*, vol. MTT-13, no. 3, pp. 379–380.
- [25] Bathker, D.A., “A Stepped Mode Transducer Using Homogeneous Waveguides.” 1967, *IEEE Trans. Microwave Theory and Techniques*, vol. 15, no. 2, pp. 128–130.
- [26] Padman, R., “Guide to the Design of Rectangular-to-Circular Waveguide Stepped Multi-Section Transitions,” 1977, Division of Radiophysics, CSIRO, Sydney, Australia, Internal Report, RPP 2121(L).
- [27] Arndt, F. and Papziner, U., “Modal S-Matrix Design of Microwave Filters Composed of Rectangular and Circular Waveguide Elements,” 1991, *IEEE MTT-S Digest*, vol. 2, pp. 535–538.

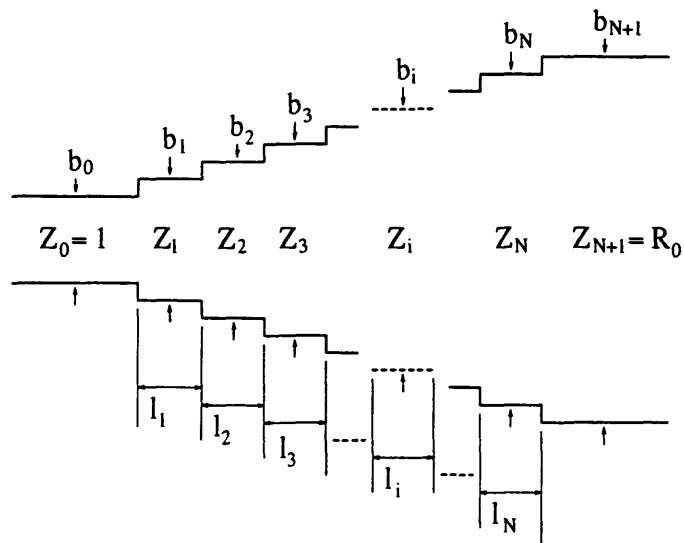


Figure 1. Stepped Waveguide Transformer

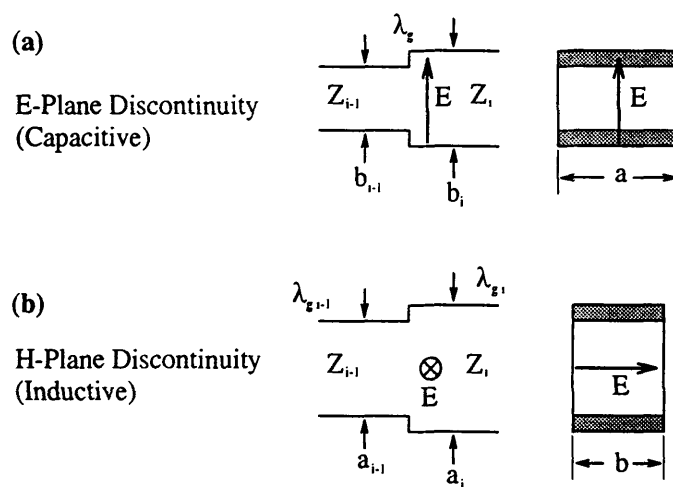


Figure 2. Rectangular Waveguide Step Discontinuities

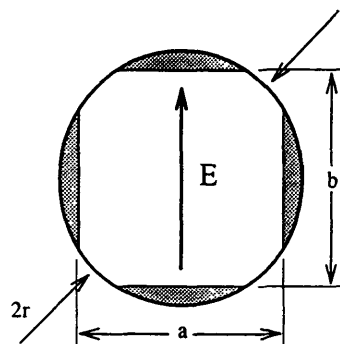


Figure 3. Stepped TE_{10}^{\square} - to - TE_{11}° Junction with Constant Radius

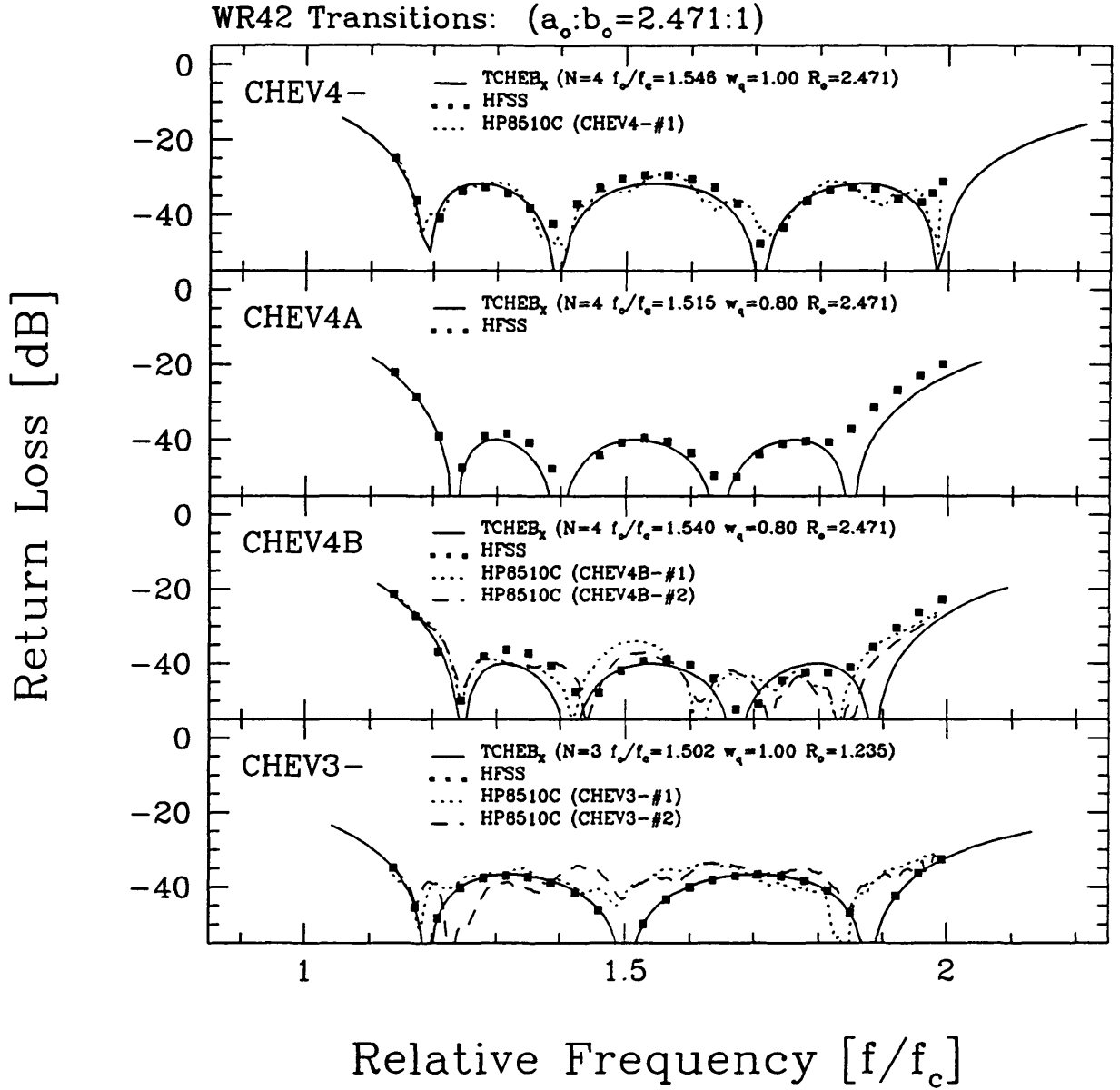


Figure 4. Measured and Computed Stepped Transformer Responses. The solid line in each panel is the design goal in the single mode limit. The square points were modeled with HFSS [6]. The dashed lines are data taken on stepped waveguide transformers with the HP8510C network analyzer. The noise floor of the TRL (Thru-Reflect-Load) calibration is < -45 dB across the band.

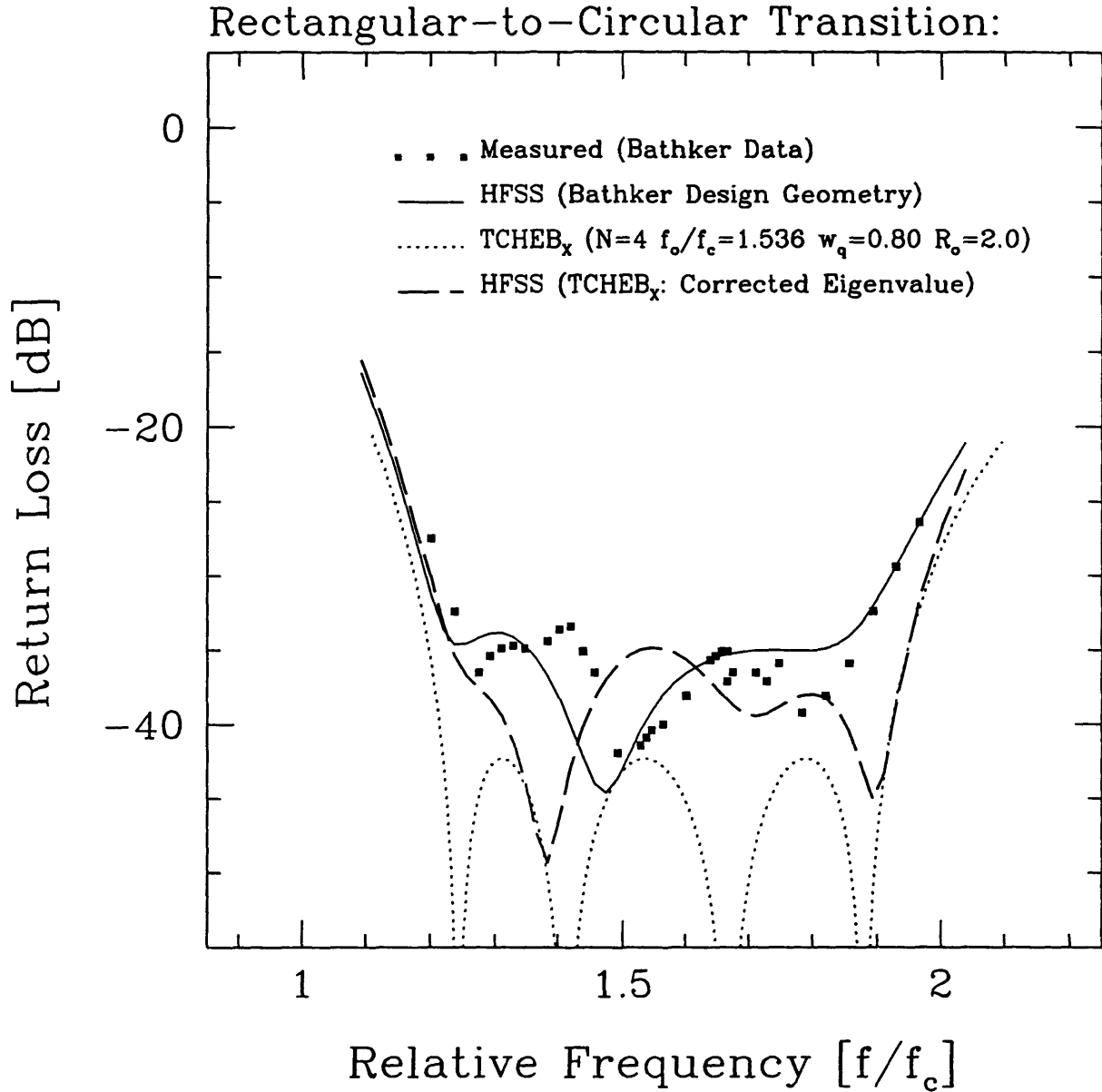


Figure 5. Circular-to-Square Transition. The solid line and square boxes are respectively the results of the finite element simulation and Bathker's measured data [25]. The long dashed line is the computed response for the corrected eigenvalue design. The short dashed line is the response of an ideal Tchebyshev taper with $N = 4$, $w_q = 0.8$, and $R_o = 2$. The discrepancy between the design goal and the modeled performance reflects the approximate nature of the synthesis used in specifying the truncated junctions.